Obrabotka metallov (tekhnologiya, oborudovanie, instrumenty) = Metal Working and Material Science. 2023 vol. 25 no. 4 pp. 61–73
ISSN: 1994-6309 (print) / 2541-819X (online)
DOI: 10.17212/1994-6309-2023-25.4-61-73

NSTU NETI

Obrabotka metallov - Metal Working and Material Science

Journal homepage: http://journals.nstu.ru/obrabotka_metallov

The influence of automatic arc welding modes on the geometric parameters of the seam of butt joints made of low-carbon steel, made using experimental flux

Egor Startsev [a, *], *Pavel Bakhmatov* [b]

Komsomolsk-na-Amure State University, 27 Lenin Avenue, Komsomolsk-on-Amur, 681013, Russian Federation

[a] https://orcid.org/0000-0002-5811-7071, egorstarts@inbox.ru; [b] https://orcid.org/0000-0002-4271-0428, mim@knastu.ru

ARTICLE INFO

Article history:
Received: 15 September 2023
Revised: 20 September 2023
Accepted: 27 September 2023
Available online: 15 December 2023

Keywords:
Submerged welding
Welding modes
Geometric parameters of the seam
The quality of the welded joint

Funding
The study was carried out with financial support from the funds of the Federal State Educational Institution of Higher Education "KNAU" under the research project No. VN001/2020 "Development of an algorithm and study of the process of programmable control of the formation of a welding/surfacing roller (including the use of additive technologies) on an automatic welding installation" (2020-2023).

Acknowledgements
Research was partially conducted at core facility "Structure, mechanical and physical properties of materials".

ABSTRACT

Introduction. The metallurgical industry in the territory of the Russian Federation has accumulated a significant amount of slags obtained during the smelting of steels and cast iron. The presence of slag dumps adversely affects the ecology of regions with metallurgical enterprises. When reducing iron from slags, the by-product becomes an oxide agglomerate, which can be considered as a flux composition for arc welding/surfacing under a layer of flux, fillers of powder wires, coatings of welding stick electrodes. **The purpose of the work** is to establish the possibility of arc welding using the flux obtained by the authors and to determine the optimal welding modes with the condition of achieving the geometric parameters of the seam according to *GOST 8713-79* and the quality of the welded joint (absence of internal defects). In this paper, butt welded joints of sheet steel *VSt3sp* with a thickness of 5 mm obtained by automatic welding under a layer of flux at direct current with forced formation of a root roller on ceramic linings using flux from recycled metallurgical slag of an electric steelmaking enterprise **are investigated**. Automatic welding of flat specimens was carried out on a tractor-type *ADF-1250* machine with a wire with a diameter of 3 mm, at a constant welding speed of 54 cm/min with varying current and arc voltage within 400–600 A and 27–37 V. **The methods of investigation:** Visual measuring and radiographic control, determination of deformation of specimens by laser scanning and computer processing of 3D models were used to evaluate the quality of welded joints. Statistical modeling in the form of a two-factor experiment was also used in the work, with obtaining adequate regression equations of the influence of welding modes on the geometric parameters of the seam: the height of reinforcement and the width of the seam on the front and back of the joint. **Results and discussion.** The possibility of obtaining welding fluxes from metallurgical slags of an electric steelmaking enterprise and its use for creating welded joints is shown. Optimal modes of arc welding of thin-walled sheet parts made of low-carbon steel with forced formation of a root roller on ceramic linings is established, ensuring the absence of internal defects in the form of pores, cracks and lacks of penetration, a minimum of residual deformations and compliance of the weld size with the requirements of the existing standard. The nominal values of the geometric parameters of the seam according to *GOST 8713-79-C4* correspond to welding mode: welding speed 54 cm/min, welding current 550 A, arc voltage 30 V. The results of the work can be applied in metallurgical electric steelmaking enterprises producing low-carbon steel in the development of technologies for the use of welding materials from slag.

For citation: Startsev E.A., Bakhmatov P.V. The influence of automatic arc welding modes on the geometric parameters of the seam of butt joints made of low-carbon steel, made using experimental flux. *Obrabotka metallov (tekhnologiya, oborudovanie, instrumenty) = Metal Working and Material Science*, 2023, vol. 25, no. 4, pp. 61–73. DOI: 10.17212/1994-6309-2023-25.4-61-73. (In Russian).

Introduction

The Russian metallurgical industry has accumulated a substantial amount of slag from iron and steel manufacturing. Steel slag waste has a detrimental effect on the local environment where metallurgical mills operate [1]. Recycling of waste steel slag piles and higher efficiency of new slag repurposing is a national growth priority [2].

*** Corresponding author**
Startsev Egor A., Senior lecturer
Komsomolsk-na-Amure State University, 27 Lenin Ave.,
681013, Komsomolsk-on-Amur, Russian Federation
Tel.: +7 (914) 188-05-45, **e-mail:** egorstarts@inbox.ru

Electric furnace steel slag waste may be utilized by the cement sector [3–10]. The overseas advanced iron and steel industry recycles all blast furnace slag and a large portion of steel slag [11, 12].

The shortage of metal scrap at *EAF* mills triggers a quest for its replacement options: use of iron ore pellets, recycling of production waste (steel slag with 60 % of iron oxide max.), etc. [13].

A mixture of oxides is a secondary product of reducing slag into iron, and it may be used as a flux compound for submerged arc welding/weld overlay, inside a flux-cored wire, or for a manual welding rod coating [14].

The chemical content of the new flux compound is mainly dictated by the slag system used by the *EAF* mill to make a specific steel grade [15–17].

The paper [18] shows the effect of flux chemical content obtained by recycling industrial waste from an *EAF* mill and additives injected into it on the structure and phase and the failure surface of submerged arc weld overlay and welds.

The authors of [19] produced a flux compound by electroslag remelting of steel slag from the *"Amurstal"* Steel Mill, crushing, and binding the components with sodium silicate. Considering the chemical content complexity of the resulting flux, and its unclear heat transfer properties, the purpose of this paper is to find the best energy parameters for submerged arc welding to achieve the normalized weld size.

The scope of the study is to determine the effect of submerged arc welding parameters using the tested flux on weld quality: the occurrence of subsurface and surface defects and weld dimensions and the type of the flux effect on the stress-strain response of the weld specimens using commercially available and tested flux.

Methods

Eight *VSt3sp* (*ASTM A570*, Gr. 36) steel sheet welded specimens with a size of 195×440×5 mm (fig. 1, *a*), having a welded joint type *S4* in accordance with *GOST 8713–79* – a single-sided single-pass square butt weld with a ceramic backing strip attached to the weld root with a metallized adhesive tape (fig. 1, *b*) were studied. The workpieces were fitted up without a gap to prevent misalignment, and temporary fixtures (100×40×5 mm, *VSt3sp* (*ASTM A570*, Gr. 36) steel) were welded by two short tack welds (10–15 mm).

The specimens were welded with a 3 mm *GOST 2246-70 Gr. Sv-08A* filler wire. A newly invented proprietary welding flux [20] with a grain size of 1.0–4.0 mm, was used as protective barrier for submerged arc welding.

Automated welding machine *ADF-1250* with power supply *VDU-1250* was used for welding at the parameters listed in table 1. Specimen 8 used as a reference was welded using the commercially available welding flux *AN-42*.

We should mention that when welding specimen 1, severe porosity caused by gas emission due to oxidation by flux melting and increased pressure in the interface between the ceramic backing and the specimen was observed. To avoid this adverse effect, 10 mm long slots at 15 mm spacing were cut in the

a *b*

Fig. 1. A specimen assembled for welding with a glued ceramic lining:

a – general view of the assembled specimen; *b* – profile of the specimen and the ceramic lining

Table 1

Automatic submerged arc welding modes

Specimen	Welding arc current, A	Arc voltage, B	Welding speed, cm/min
1	600	37	54
2	600	37	
3	500	37	
4	400	37	
5	450	37	
6	450	27	
7	500	27	
8	500	27	

foil tape longitudinally at the interface between the ceramic backing and the workpiece surface in other specimens. Therefore, specimens 1 and 2 in table 1 have the same parameters.

Welds were visually inspected as described in *STO 9701105632-003-2021* with magnifying glass *LI-10*, caliper, and welder's gauge *UShS-3*.

Welds were radiographically inspected as required by *GOST ISO 17636-1-2017* by using a radiation source, X-ray system *PION-2M*, X-ray film *Agfa D4*, a source-to-film distance of 350 mm, exposure time of 10 sec., and radiographic technique 1.

Strain behavior of welded specimens was measured based on its digital twins obtained by *MCAx* laser scanning and 3D model processing with the *Focus 10* Inspection software.

We used the *Microsoft Excel* analysis package for statistical modeling. Relationship between input parameters (welding current X_1 and arc voltage X_2) and output parameters (weld cap height and weld root bead height and weld cap width and root bead width) was found. Basic value of the variables was determined by experiment assuming the arc process stability at welding a full-size weld.

Results and discussion

Welding of the specimens with the tested flux produced a gentle, silent arcing, no fumes, and easy post-weld removal of the hardened slag layer.

The appearance of the resulting welded specimens is shown in fig. 2. Visual inspection showed the following: all specimens had a properly formed weld bead with no surface defects at the weld's face. On the reverse side in Sample 1, discontinuities are observed with a width of 1.5–2.0 mm, a depth of 1.0–1.5 mm and an average length of 10 mm, located mainly at the start and central part of the weld. Weld root was formed against the surface of the ceramic backing with a vigorous interaction with its material, and therefore the bead surface does not replicate the smooth surface shape of the backing. The root bead in Specimen 2 also has discontinuities at the start of the weld with a depth of 0.2–0.5 mm, a width of 1.5–2.0 mm, and an average length of 5 mm. Specimen 3 does not have any surface defects in the root bead that are common to Specimen 1 and 2, but its surface was shaped in the same way. The welding parameters used for Specimen 4 were inadequate to achieve the required root bead size at the start of the weld. Penetration stabilized in the center of the weld, but the root bead was welded unsupported, failing to contact the surface of the ceramic backing. The surface of Specimen 5 is similar to that of Specimen 3. Specimens 6 to 8 have a clear pattern of ceramic backing segments with a smooth surface at the root bead and are perfectly sized to match the configuration of the backing's supporting part.

Therefore, to weld 5 mm thick mild steel sheets with the tested flux, the welding parameters of 400 A/37 V are inadequate for forming the root bead, and 600–500 A/37 V are excessive in energy and cause melting of the backing material and vigorous interaction with the molten weld pool, gas emission, and the occurrence of defects such as discontinuities. The best welding parameters are 450–500 A/27 V.

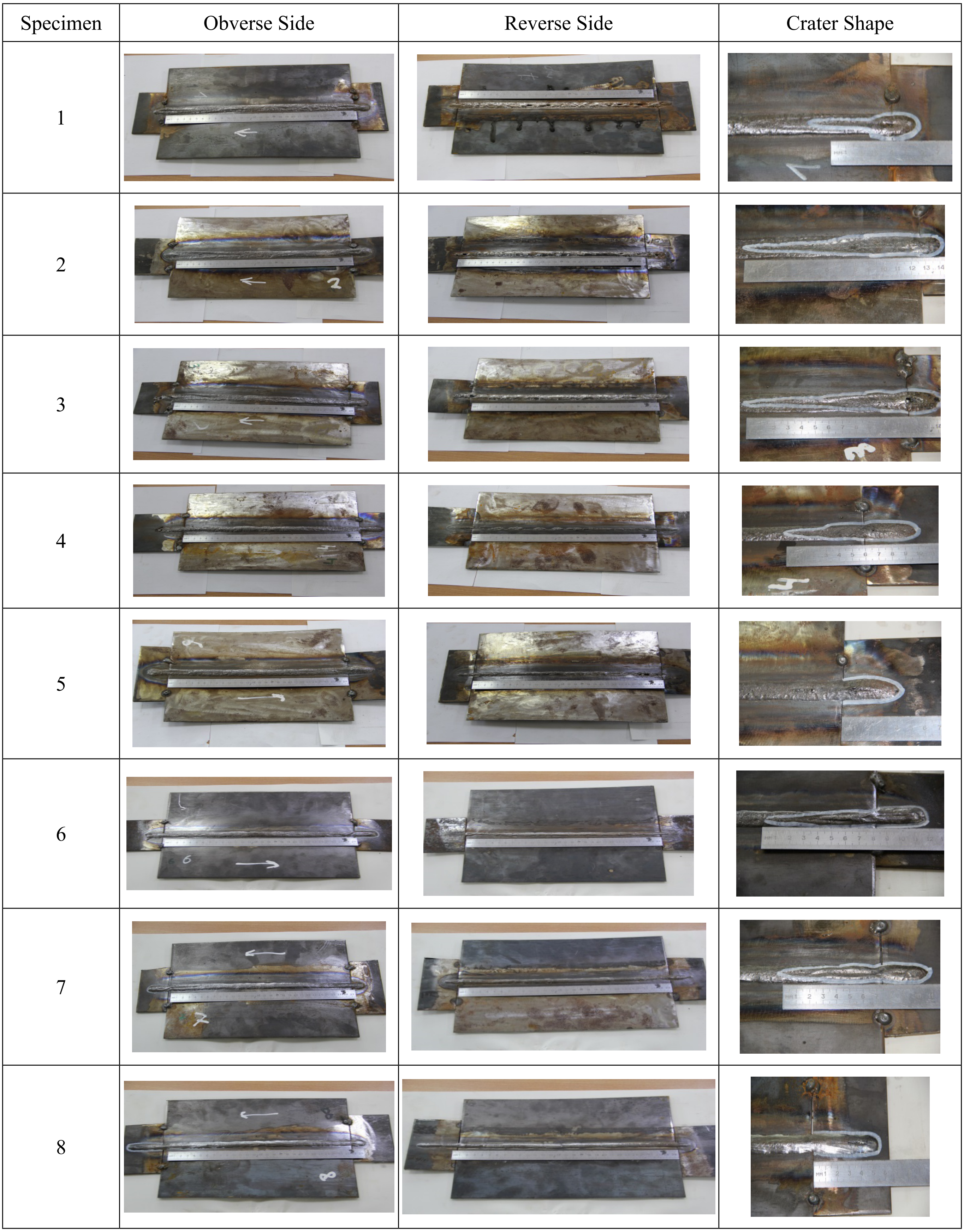

Fig. 2. Appearance of the resulting welded specimens

Almost all specimens welded using the tested flux with all the welding parameters had an elongated crater with an average length of 100–110 mm and a depth of 1–1.5 mm, which is approximately twice the length of the weld crater occurring when using commercially available flux or 6 mm (Specimen 8). A higher heat capacity of the tested flux may attribute to it. Crater concavity suggests a higher density of the tested flux that interferes with the release of superheated gas and metal vapor pressure below the flux layer above the weld pool when the arc is stopped.

Table 2 shows the *GOST 8713-79-S4* weld size measurements for the specimens for a welded piece with a thickness of 5 mm.

Table 2

Results of visual and dimensional inspection

GOST 8713-79-S4 (for 5 mm thick workpieces)			
Weld cap width e, mm	≤ 23		
Root bead width e_1, mm	12 ± 4		
Weld cap height g, mm	1.5 ± 1.0		
Root bead height g_1, mm	1.5 ± 1.0		
Specimen 1 (600 A, 37 V)			
Measurement point	Start	Center	End
Weld cap width e, mm	17.5	15.9	18.6
Root bead width e_1, mm	18.3	16.3	17.5
Weld cap height g, mm	2	1	3
Root bead height g_1, mm	1	1	1
Specimen 2 (600 A, 37 V)			
Measurement point	Start	Center	End
Weld cap width e, mm	17	18	17
Root bead width e_1, mm	14.2	13.5	13.8
Weld cap height g, mm	1.5	0	0.5
Root bead height g_1, mm	3	4	4
Specimen 3 (500 A, 37 V)			
Measurement point	Start	Center	End
Weld cap width e, mm	16.5	17.4	16.6
Root bead width e_1, mm	12.1	11	13.5
Weld cap height g, mm	2.5	2	2
Root bead height g_1, mm	0	1	1
Specimen 4 (400 A, 37 V)			
Measurement point	Start	Center	End
Weld cap width e, mm	14.4	14	14.2
Root bead width e_1, mm	Lack of penetration	5.5	7
Weld cap height g, mm	1	2	1
Root bead height g_1, mm	Lack of penetration	1.5	1.5
Specimen 5 (450 A, 37 V)			
Measurement point	Start	Center	End
Weld cap width e, mm	15.7	15	15.8
Root bead width e_1, mm	9.8	9	8.9
Weld cap height g, mm	0	0.5	0
Root bead height g_1, mm	1	2	0

The End Table 2

GOST 8713-79-S4 (for 5 mm thick workpieces)			
Specimen 6 (450 A, 27 V)			
Measurement point	Start	Center	End
Weld cap width *e*, mm	12.4	12.5	12.4
Root bead width e_1, mm	8	8	8.6
Weld cap height *g*, mm	1.5	1	1
Root bead height g_1, mm	0.5	0.5	0.5
Specimen 7 (500 A, 27 V)			
Measurement point	Start	Center	End
Weld cap width *e*, mm	11.7	12.5	11.2
Root bead width e_1, mm	14.7	9.3	9.9
Weld cap height *g*, mm	2	2	2
Root bead height g_1, mm	1	1	0.5
Specimen 8 (500 A, 27 V) (commercially available flux)			
Measurement point	Start	Center	End
Weld cap width *e*, mm	13.4	13.1	13.6
Root bead width e_1, mm	10.6	10.2	9.2
Weld cap height *g*, mm	1	2	2
Root bead height g_1, mm	1	0.5	1
Note: (green) — acceptable	(red)	— unsatisfactory characteristics	

Table 2 shows that Specimens 1–5 fail to meet the *GOST 8713-79* size requirements for weld type *S4*. Other Specimens 6–8 satisfy all of the above requirements.

Radiographs of the resulting weld specimens are shown in fig. 3.

Radiographic inspection of the welds (fig. 3) revealed the defects in specimen 1, 2, and 5 (discontinuities) that had been earlier detected by visual inspection. Specimen 4 had a 17 mm long lack of fusion at the start of the weld. Except for the above irregularities, all the specimens have solid weld metal with no hidden subsurface defects (porosity or cracking).

Fig. 4 shows the computer processing results for the 3D weld specimen models generated by laser scanning and demonstrating its overall residual strain profile.

Fig. 4 shows that Specimens 1 and 3–8 have a common longitudinal strain that is evident from an upward curvature of the specimen face that is highest at the cross section of the weld's center, while Specimens 2 and 5 have a downward curvature in the weld root direction. Specimen 2 shows a higher lateral strain that is highest at the start and end of the weld. Specimens 3 and 6 show twisting distortion, that is, the cross section is twisted around the longitudinal centerline due to the hybrid nature of the strain.

Strain is lowest in Specimens 4 and 6–8. Strain behavior of Specimens 4 and 8 is similar with respect to the maximum strain area width. Specimen 6 shows the best performance.

Consequently, high arc energy (600 A/37 V, (2,466 kJ/mm)) using the tested flux causes both longitudinal and lateral strain with a max. deflection of 5 mm. An intermediate energy input of 500 A/37 V (2,055.5 kJ/mm) results in an intricate strain rate pattern combining both longitudinal and lateral strain. 400 A/37 V (1,645 kJ/mm) produced lowest longitudinal strain and an unsatisfactory weld root formation. The best welding parameters for 5 mm thick sheet pieces using the tested flux with a ceramic backing are 450 A/27 V (1,350 kJ/mm) that will form a good bead both on the face and root to meet *GOST 8713-79-S4* and minimize the residual strain of the welded component.

Table 3 summarizes statistical modeling of the welding parameters effect on the resulting weld size using the tested flux.

Specimen	X-ray pattern	Defect according to *GOST 7512-82*
1	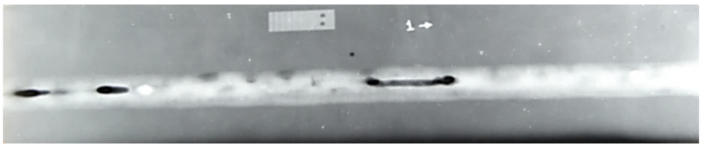	*B20*×2; 2*B10*×2; Σ30
2	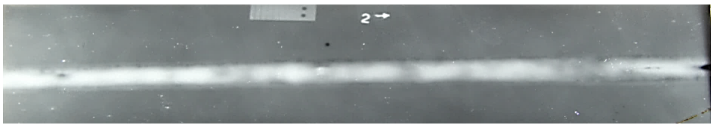	*A*1.5; *D10*×0.3
3	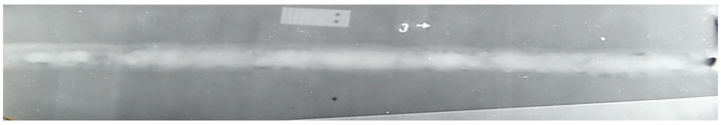	None discovered
4	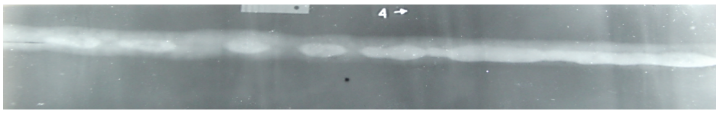	*D17*×0.5
5	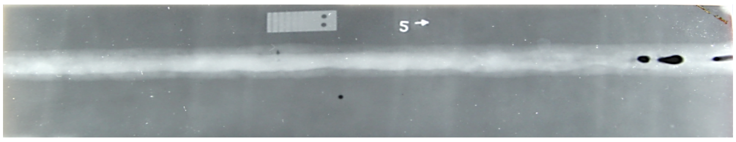	*B5*×2; *B10*×2; Σ15
6	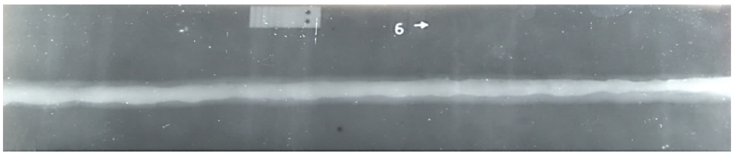	None discovered
7	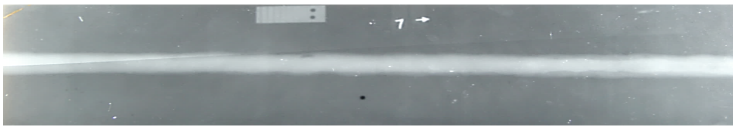	None discovered
8	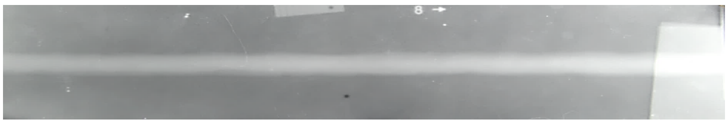	None discovered
Notice: the arrow on the X-ray pattern indicates the direction of welding		

Fig. 3. X-ray patterns of welded specimens

The calculated regression equations were used to plot the weld size vs welding parameters curves (fig. 5).

An increase in the arc voltage does not have such a significant increase in the weld cap width on the front side, as an increase in the current. And vice versa, a higher voltage increases the root bead width, and a higher welding current has no effect on this variable (fig. 5,a).

As it can be seen in fig. 5,b, the selected welding parameters range of 400–600 A and 25–40 V has practically no effect on the weld cap height, but a substantial effect on the increase in the root bead height.

A set of four regression equations was solved to find the best welding parameters to achieve the normal weld size, that is, 550 A, 30 V.

Conclusion

1. The newly invented and tested flux will produce welds with minimal residual strain and free from hidden subsurface defects.

2. When welding 5 mm thick pieces using the tested flux with a ceramic backing, arc energy (600 A/37 V, (2,000–2,466 kJ/mm)) appears to be excessive and causes a vigorous interaction between the weld pool and the backing material and results in both longitudinal and lateral strain with a deflection of 5 mm.

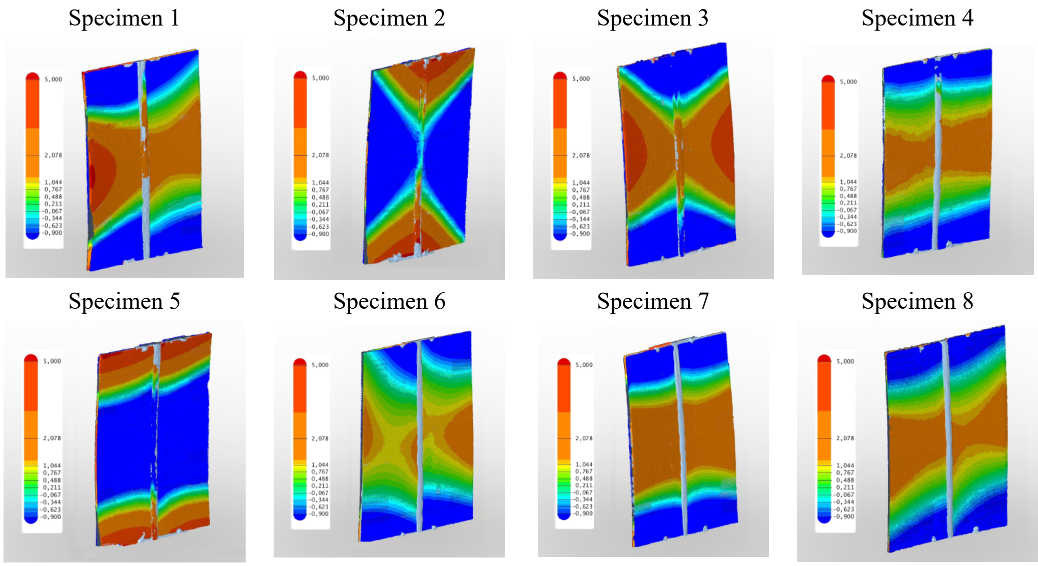

Fig. 4. Deformation pattern of welded specimens

Table 3

The result of a two-factor experiment

Iteration No.	X_1	X_2	Weld cap width	Root bead width	Weld cap height	Root bead height
1	600	37	15.9	16.3	1	1
2	600	37	18	13.5	0	4
3	500	37	17.4	11	2	1
4	400	37	14	5.5	0.5	2
5	450	37	15	9	0.5	2
6	450	27	12.5	8	1	0.5
7	500	27	12.5	9.3	2	1
8	500	27	13.1	10.2	2	0.5
Regression equation			$Y = 1.52 + 0.01X_1 + 0.253X_2$	$Y = -12.62 + 0.0445X_1 + 0.0225X_2$	$Y = 2.44 + 0.0008X_1 - 0.054X_2$	$Y = -2.55 + 0.0025X_1 + 0.0875X_2$

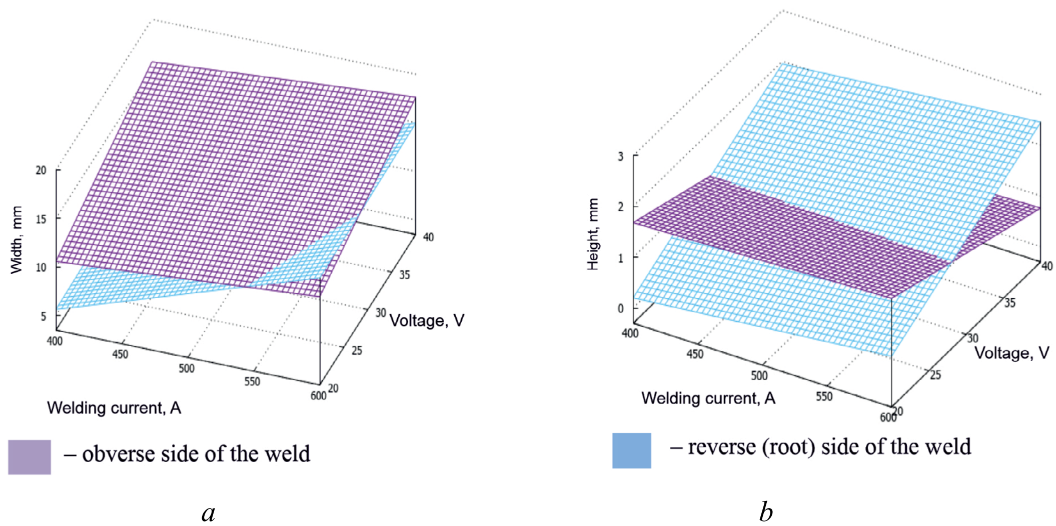

Fig. 5. Graphs of the dependence of the width (a) and the height of the reinforcement (b) of the seam from the regression equations for welding plates with a thickness of 5 mm on the welding modes

400 A/37 V produced lowest longitudinal strain and an unsatisfactory weld root formation. The best welding parameters are 450 A/27 V (1,350 kJ/mm) that will form a good bead both on the face and root to meet *GOST 8713-79-S4* and minimize the residual strain of the welded component.

3. It is found that a higher arc voltage results in a larger root bead width and has little effect on the weld cap width. In contrast, a higher welding current increases the weld cap width and has no effect on the root bead width. The selected welding parameters range of 400–600 A and 25–40 V has no effect on the weld cap height, but a substantial effect on the root bead height.

It is determined the best welding parameters for butt welds of a 5 mm thick mild steel sheet to achieve the normal weld size as required by *GOST 8713-79-S4*, that is, a travel speed of 54 cm/min, a welding current of 550 A, and an arc voltage of 30 V.

References

1. Verkhoturov A.D., Babenko E.G., Makienko V.M. *Metodologiya sozdaniya svarochnykh materialov* [Methodology of creation of welding materials]. Khabarovsk, Far Eastern State Transport University Publ., 2009. 128 p. ISBN 978-5-262-00458-4.

2. Sviridova T.V., Bobrova O.B., Peryatinsky A.Yu., Nekerov E.A. Evaluation of the influence of slag heaps on the state of the urban residential area. *IOP Conference Series: Materials Science and Engineering*, 2019, vol. 537 (6). DOI: 10.1088/1757-899X/537/6/062009.

3. Khamatova A.R., Khohryakov O.V. Elektrostaleplavil'nyi shlak OAO «Izhstal'» dlya tsementov nizkoi vodopotrebnosti i betonov na ikh osnove [The electro-steel-smelting slag JSC "Izhstal" for cements of low water demand and concrete on their basis]. *Izvestiya Kazanskogo gosudarstvennogo arkhitekturno-stroitel'nogo universiteta = News KSUAE*, 2016, no. 2 (36), pp. 221–227.

4. Tsakiridis P.E., Papadimitriou G.D., Tsivilis S., Koroneos C. Utilization of steel slag for Portland cement clinker production. *Journal of Hazardous Materials*, 2008, vol. 152 (2), pp. 805–811. DOI: 10.1016/j.jhazmat.2007.07.093.

5. Wu Chzhan. *Mixed slag smelting reduction production and thermal refining method*. Patent of China, no. 201610570916, 2018.

6. Albuquerque Contrucci M., Marcheze E.S. *Method for the use of electric steel plant slag for self-reducing agglomerates*. Patent US, no. 6391086, 2002.

7. Krofchak D. *Method of making cement or mine backfill from base metal smelter slag*. Patent US, no. 6033467, 2000.

8. Edlinger A. *Method of manufacturing pig iron or steel and cement clinker from slags*. Patent US, no. 5944870, 2016.

9. Song Q., Shen B., Zhou Z. Effect of blast furnace slag and steel slag on cement strength, pore structure and autoclave expansion. *Advanced Materials Research*, 2011, vol. 168–170, pp. 17–20. DOI: 10.4028/www.scientific.net/AMR.168-170.17.

10. Skaf M., Manso M.J., Aragon A., Fuente-Alonso J.A., Ortega-López V. EAF slag in asphalt mixes: A brief review of its possible re-use. *Resources, Conservation and Recycling*, 2017, vol. 120, pp. 176–185. DOI: 10.1016/j.resconrec.2016.12.009.

11. Yung V.N., Butt Yu.M., Zhuravlev V.F., Okorokov S.D. *Tekhnologiya vyazhushchikh veshchestv* [Technology of binders]. Moscow, Gosstroiizdat Publ., 1952. 600 p.

12. Laskorin B.N., Gromov B.V., Tsygankov A.P., Senin V.N. *Problemy razvitiya bezotkhodnykh proizvodstv* [Problems of development of waste-free production]. Moscow, Stroiizdat Publ., 1981. 207 p.

13. Bakhmatov P.V., Startsev E.A., Grigor'ev V.V., Bryanskii A.A. Scrap deficit problem at the Amurstal metallurgical plant and search for alternatives to substitute it. *Metallurgist*, 2022, vol. 66 (3), pp. 376–382. DOI: 10.1007/s11015-022-01339-6.

14. Belskii S.S., Zaitseva A.A., Tyutrin A.A., Ismoilov Z.Z., Baranov A.N., Sokolnikova Yu.V. Current state of steelmaking slag processing. *iPolytech Journal*, 2021, vol. 25 (6), pp. 782–794. DOI: 10.21285/1814-3520-2021-6-782-794.

15. ITS 26–2017. *Informatsionno-tekhnicheskii spravochnik po nailuchshim dostupnym tekhnologiyam. Proizvodstvo chuguna, stali i ferrosplavov* [ITS 26-2017. Information and technical guide to the best available technologies. Production of pig iron, steel and ferroalloys]. Moscow, Byuro NTD Publ., 2017. 478 p.

16. Kozyrev N.A., Kryukov R.E., Kryukov N.E., Koval'skii I.N., Usol'tsev A.A. Razrabotka novykh svarochnykh flyusov i flyus-dobavok dlya svarki i naplavki stali na osnove tekhnogennykh otkhodov metallurgicheskogo proizvodstva [Development of new welding fluxes and flux-additives for welding and surfacing steel on basis of technogenic wastes of metallurgical production]. *Zagotovitel'nye proizvodstva v mashinostroenii = Blanking productions in mechanical engineering*, 2017, vol. 15 (6), pp. 249–254.

17. Kozyrev N.A., Kryukov R.E., Mikhno A.R., Usoltsev A.A., Umanskiy A.A. Razrabotka novykh svarochnykh flyusov na osnove shlaka silikomargantsa i kovshevogo elektrostaleplavil'nogo shlaka [Development of new welding fluxes based on silicomanganese slag and ladle electric steel-smelting slag]. *Svarochnoe proizvodstvo*, 2020, no. 2, pp. 16–21. (In Russian).

18. Kryukov R.E., Gromov V.E., Kozyrev N.A., Ivanov Yu.F., Shlyarova Yu.A. *Strukturno-fazovye sostoyaniya i poverkhnost' razrusheniya elektrodugovoi naplavki i svarnykh shvov* [Structural-phase states and fracture surface of electric arc surfacing and welds]. Novokuznetsk, SibGIU Publ., 2022. 136 p. ISBN 978-5-7806-0585-0.

19. Bakhmatov P.V., Startsev E.A., Sobolev B.M. Impact and effect study of submerged-arc welding conditions on structural changes in weld metal. *Lecture Notes in Networks and Systems*, 2021, vol. 200, pp. 65–76. DOI: 10.1007/978-3-030-69421-0_8.

20. Bakhmatov P.V., Startsev E.A., Gladovskij R.E., Sobolev B.M. *Sposob izgotovleniya svarochnogo flyusa iz tekhnogennykh otkhodov staleplavil'nogo proizvodstva* [Method for manufacturing welding flux from man-made waste of steelmaking]. Patent RF, no. 2022128798, 2023.

Conflicts of Interest

The authors declare no conflict of interest.